

# Influence of Heat Source on Thin Film Flow of Ferrofluid Past an Unsteady Stretching Sheet

B. Azghar Pasha<sup>1\*</sup>, G. Sowmya<sup>1</sup>, V. Ramachandramurthy<sup>2</sup> and H. M. Nagesh<sup>3</sup>

<sup>1</sup>Department of Mathematics, M. S. Ramaiah Institute of Technology, Bengaluru - 560054, Karnataka, India; [azgharpasha@msrit.edu](mailto:azgharpasha@msrit.edu)

<sup>2</sup>Department of Basic Sciences, R. R. Institute of Technology, Bengaluru - 560090, Karnataka, India

<sup>3</sup>Department of Science and Humanities, PES University - Electronic City Campus, Bengaluru - 560100, Karnataka, India

## Abstract

In this work, the impact of a heat source on the thin-film ferrofluid flow over an unstable stretching sheet in the presence of an external magnetic field has been examined. The governing partial differential equations are transformed into a system of ordinary differential equations by similarity transformation. The resultant system of ordinary differential equations is solved numerically through shooting technique involving Runge-Kutta-Fehlberg (RKF45) method. To improve the initial guess values, the Newton-Raphson method is used. The significance of magnetization parameter, Prandtl number and heat source parameter on the flow and heat transmission process have been graphically analysed. The decrease in film thickness is observed for growing values of heat source parameter.

**Keywords:** Heat Source, Stretching Sheet, Thin Film

## 1.0 Introduction

Due to the enormous application of flow of thin film on an elastic surface in the field of manufacturing industries, coating process, chemical process, steel industries, metal casting, process of polymer extrusion, etc., which gain the attention of many researchers. Most of the flow issues pertinent to the polymer expulsion process are actuated by the stretching movement of the flat elastic sheet. Considering these applications, Crane<sup>1</sup> was first to concentrate on the stretching sheet issue in which the velocity was expected to change linearly from the slit. Andersson<sup>2</sup> obtained the exact solution for the flow of viscous fluid over a stretching sheet under magnetic field condition. Andersson *et al.*<sup>3</sup> have addressed the transfer of heat in a time-dependent elastic sheet having laminar

liquid film on it. Viscous flow across a nonlinear sheet has been proposed by Vajravelu<sup>4</sup> and he demonstrated that heat flow is always from stretching sheet to the fluid. Numerical investigation on thin film on a stretching sheet has been described by Dandapat *et al.*<sup>5</sup>. They show that viscosity of the fluid has positive impact on thin film thickness. Khan *et al.*<sup>6</sup> explored the heat transmission characteristics of thin film for second-grade fluid in a porous medium. They show that porosity parameter reduces the velocity profile. Newtonian fluid flow on a horizontal sheet has been illustrated by Safdar *et al.*<sup>7</sup> considering smoothness of the liquid film surface. The flow and thermal distribution augments with unsteadiness.

The analysis of magnetic field also attracted many researchers due to its wide spread applications in many engineering disciplines. In this regard, Khan *et al.*<sup>8</sup>

\*Author for correspondence

explores the stagnation point flow across a stretching sheet considering ferro particles. It is obtained that velocity profile increases with higher stretching parameter. Qasim *et al.*<sup>9</sup> exhibit unsteady thin film flow across a stretching sheet. They remarked that free surface temperature increases with magnetic parameter. Ferrofluid flow across a variable thickness surface has been examined by Ramana Reddy *et al.*<sup>10</sup>. This work explores that surface thickness is the reason behind reduced velocity field. Krishanan *et al.*<sup>11</sup> considered unsteady porous stretching sheet with magnetic field to study the heat transfer. They remarked in their work that the thickness of the liquid film tends to increase for Hartmann number and injection velocity.

The ferrofluids address a class of magnetizable fluids with fascinating properties equipped for significantly effecting on technology. In numerous business applications, ferrofluid is a fundamental part of the framework which upgrades the performance. Ferrofluids are used in a broad variety of industries, including electronic packaging, magnetic sealing, biotechnology, aerospace, medicine and many more. Hence, several researchers have investigated on this topic some of them are mentioned here. Andersson and Valnes<sup>12</sup> have examined the effect of magnetic dipole on the viscous ferrofluid flow over an elastic sheet. Magneto-thermo mechanical interaction due to ferromagnetic liquid stream was studied by Narayana *et al.*<sup>13</sup>. It is obtained that fluid velocity declines with magneto-thermo mechanical interaction. Jalili *et al.*<sup>14</sup> scrutinized the ferrofluid flow over a stretching sheet considering magnetic field. It is noted that magnetic parameter and flow distribution has inverse relation. Bhandari and Husain<sup>15</sup> have discussed about the combined impact of rotational viscosity as well as magnetization force on the flow of ferrohydrodynamic nanoliquid past an elastic sheet with the help of Shliomis model.

The stretching sheet's temperature and velocity distribution is influenced by the presence of a heat source. Thus, the effects of a non-uniform heat source and viscous dissipation on the flow of a viscoelastic fluid over a stretching sheet have been discussed by Abel *et al.*<sup>16</sup>. Abel and Mahesha<sup>17</sup> have analytically studied the significance of non-uniform heat source and thermal radiation effect on the flow of magnetohydrodynamic viscoelastic fluid past a surface of flat sheet by regular perturbation method. Zheng *et al.*<sup>18</sup> explored the boundary layer flow across a permeable sheet with the influence of heat source and sink.

The velocity of the fluid retards as the value of suction/injection increases. The role of rotating magnetic field and heat generation/absorption has been emphasized by Majeed *et al.*<sup>19</sup>. It is inferred that the interaction between magnetic, mechanical and thermal component declines flow velocity. Aslani *et al.*<sup>20</sup> have examined the influence of heat source/sink, viscous dissipation, radiation and partial slip on the heat transfer through the flow of liquid film over a porous elastic sheet.

In view of the above-mentioned literature survey, we planned to examine the significances of the heat source parameter on the flow of the ferromagnetic liquid thin film on an elastic surface under transient condition. The obtained partial differential equations are converted to ordinary differential equations through the use of similarity transformations. The influence of dimensionless constraints on the velocity distribution, thermal performance, wall temperature gradient, free surface velocity and temperature have been illustrated graphically.

## 2.0 Mathematical Formulation

A flow of a thin ferromagnetic liquid film on an elastic sheet at  $\mathbf{y} = \mathbf{0}$  emerging out of a narrow slit is considered in the present analysis and is as shown in Figure 1. Here, the film thickness  $h(t)$  which varies with time is assumed to be uniform. The fluid movement is begun by the extending of the sheet by the act of two equivalent and opposite forces along  $x$ -direction. The velocity of the stretching sheet is considered to be of the form

$$U(x, t) = \frac{bx}{1-\alpha t}, \quad (1)$$

where, the constants  $\alpha$  and  $b$  are constants such that  $0 \leq \alpha < 1$ .

Here,  $\frac{b}{1-\alpha t}$  represents the rate of effective stretching and it rises with time.

A magnetic field  $\vec{H} = (H_1(t, x, y), 0, 0)$  is applied in the path of the extending sheet. The surface temperature  $T_s$  of the elastic sheet is defined as follows:

$$T_s = T_c - \left\{ \frac{bx^2}{2\nu(1-\alpha t)^{3/2}} \right\} T_{ref}, \quad (2)$$

Here,  $T_c$  represents the curie temperature, beyond which the magnetic properties of ferrofluid ceases to exist and hence the temperature is maintained below  $T_c$ .  $T_{ref}$  is the reference temperature so that  $0 \leq T_{ref} \leq T_c$ . From equation (1) it is clear that the surface temperature  $T_s$  which is a function of  $t$  and  $x$  diminishes with time.

Here, it is assumed that, the thermal conductivity, heat capacity and viscosity are constants. Also, the influence of viscosity and surface tension on the magnetization vector  $\vec{M} = (M_1(t, x, y), 0, 0)$ , which is directed along the sheet is presumed to be negligible. With this consideration, the governing equations of flow takes the below form

$$\frac{\partial u}{\partial x} + \frac{\partial v}{\partial y} = 0, \tag{3}$$

$$\frac{\partial u}{\partial t} + u \frac{\partial u}{\partial x} + v \frac{\partial u}{\partial y} = \nu \frac{\partial^2 u}{\partial y^2} - \frac{\mu_0}{\rho} M_1 \frac{\partial M_1}{\partial x}, \tag{4}$$

$$\frac{\partial T}{\partial t} + u \frac{\partial T}{\partial x} + v \frac{\partial T}{\partial y} = \frac{k}{\rho C_{vh}} \frac{\partial^2 T}{\partial y^2} + \frac{1}{\rho C_{vh}} \frac{Q_0(T - T_c)}{(1 - \alpha t)}, \tag{5}$$

where,  $\nu = \frac{\mu}{\rho}$ , is the kinematic viscosity. The boundary conditions below are used to solve the aforementioned system of equations:

$$u = U, v = 0, T = T_s \text{ at } y = 0, \tag{6}$$

$$\frac{\partial u}{\partial y} = \frac{\partial T}{\partial y} = 0 \text{ at } y = h, \tag{7}$$

$$v = \frac{dh}{dt} \text{ at } y = h. \tag{8}$$

The displacement currents, viscous dissipation and heating due to magnetostriction are neglected while constructing the above boundary layer equations.

The similarity variables are considered in the following form so that the boundary layer equations get converted to a system of ordinary differential equations.

$$f(\eta) = \frac{\psi(t, x, y)}{\left(\frac{bv}{1-\alpha t}\right)^{\frac{1}{2}} x}, \theta(\eta) = \frac{T_c - T(t, x, y)}{T_{ref} \left\{ \frac{bx^2}{2\nu(1-\alpha t)^{\frac{3}{2}}} \right\}}, \eta = \left\{ \frac{b}{v(1-\alpha t)} \right\}^{1/2} y. \tag{9}$$

The component  $M_1$  of the magnetization vector is selected in the following form

$$M_1 = K_0 x^{-1} (1 - \alpha t)^{\frac{1}{2}} (T_c - T), \tag{10}$$

where,  $K_0$  is the pyromagnetic coefficient.

With the above choice of the similarity factors, the velocity terms can be expressed in terms of stream function as given below.

$$u = \frac{\partial \psi}{\partial y} = \left( \frac{bx}{1 - \alpha t} \right) f'(\eta), \tag{11}$$

$$v = -\frac{\partial \psi}{\partial x} = -\left( \frac{bv}{1 - \alpha t} \right)^{\frac{1}{2}} f(\eta). \tag{12}$$

Using equations (9)-(12) in the governing equations and boundary conditions (3)-(8), we get

$$S \left( \frac{n}{2} f'' + f' \right) + (f')^2 - ff'' = f''' - K^* \theta^2, \tag{13}$$

$$Pr \left[ \frac{S}{2} (\eta \theta' + 3\theta) + 2f'\theta - f\theta' \right] = \theta'' + Q^* \theta, \tag{14}$$

$$f(0) = 0, f'(0) = 1, \theta(0) = 1, \tag{15}$$

$$f''(\beta) = 0, \theta'(\beta) = 0, \tag{16}$$

$$f(\beta) = \frac{S\beta}{2}. \tag{17}$$

where

$$Pr = \frac{\mu C_{vh}}{k}, \text{ the Prandtl number,}$$

$$K^* = \frac{\mu_0}{\rho} \left( \frac{K_0}{2\nu} \right)^2 T_{ref}^2, \text{ the magnetization parameter,}$$

$$Q^* = \frac{Q_0 \nu}{bk}, \text{ the heat source parameter,}$$

$$S = \frac{\alpha}{b}, \text{ the non-dimensional unsteadiness parameter,}$$

$$\beta = h \left\{ \frac{b}{v(1 - \alpha t)} \right\}^{1/2}, \text{ the dimensionless film thickness.}$$

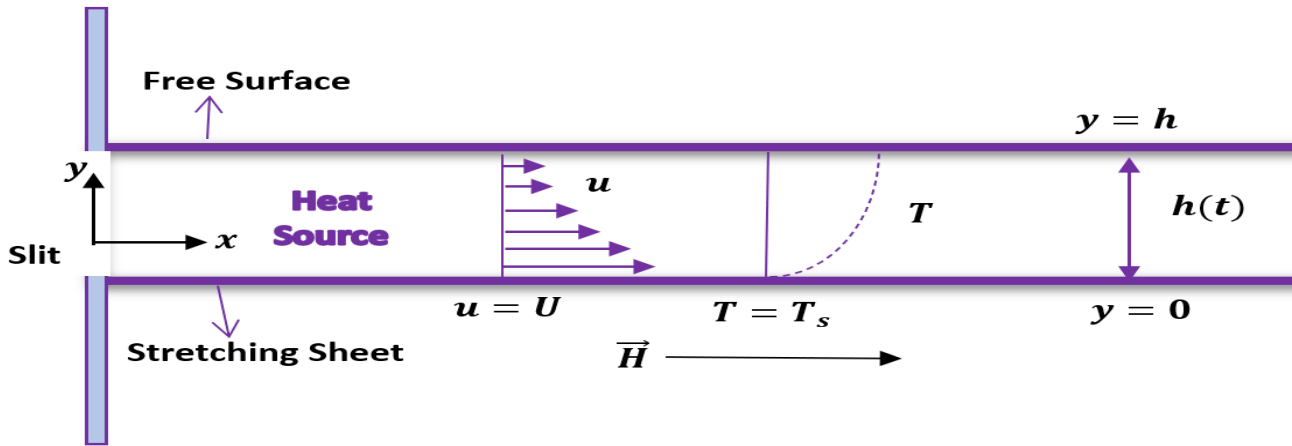


Figure 1. Schematic illustration of flow configuration.

### 3.0 Solution Procedure

Similarity transformation equation (9) is used to reduce the governing equations (3)-(5) to a system of ODEs (13)-(14). This boundary value problem is computed by shooting method which primarily converts the BVPs to IVPs by finding the missing initial condition suitably as given below

$$\frac{dA_1}{d\eta} = A_2, A_1(0) = 0 \quad ,$$

$$\frac{dA_2}{d\eta} = A_3, A_2(0) = 1 \quad ,$$

$$\frac{dA_3}{d\eta} = S \frac{\eta}{2} A_3 + A_2 + A_2^2 - A_1 A_3 + K^* A_4^2, A_3(0) = b_1,$$

$$\frac{dA_4}{d\eta} = A_5, A_4(0) = 1 \quad ,$$

$$\frac{dA_5}{d\eta} = Pr \left[ \frac{S}{2} (\eta A_5 + 3A_4) + 2A_2 A_4 - A_1 A_5 \right], A_5(0) = b_2.$$

The obtained IVPs are simplified by Runge-Kutta-Fehlberg (RKF45) method. The initial slopes  $b_1$  and  $b_2$  values are further refined using Newton-Raphson scheme. The value of the film thickness  $\beta$  is found on the basis of condition (17) and the corresponding solution to this specific value of  $\beta$  is noted and examined. The solution is obtained numerical with  $10^{-6}$  precision.

### 4.0 Results and Discussion

In this study, the influence of heat source on the thin film of the ferromagnetic liquid flow over a time-dependent elastic surface have been discussed by considering the magnetic field effect. The modelled equations have been converted to ODE's using similarity transformations and then simplified by shooting technique. The consequences of dimensionless constraints on the flow and heat transference phenomenon have been presented through Figures 2-13.

The fluctuation in the velocity profile for diverse values of the unsteadiness parameter while keeping other constraints constant has been disclosed in Figure 2. This shows that as the  $S$  value rises, the film thickness decreases, thus the freestream velocity is reached quickly. Furthermore, the unsteadiness parameter increases the velocity distribution.

The effect of heat source parameter on the velocity profile has been depicted in Figures 3 and 4 for different values of  $S$ , respectively, considering  $Pr$  and  $K^*$  to be constant. The variation in velocity distribution is minimal and it is observed that rise in the heat source parameter initially reduces the velocity profile, but an inverse trend is visible near the free stream region. Additionally, increasing the heat source parameter decreases the thickness of the thin film.

The impact of the simultaneous variation of the Prandtl number and the unsteadiness parameter on the

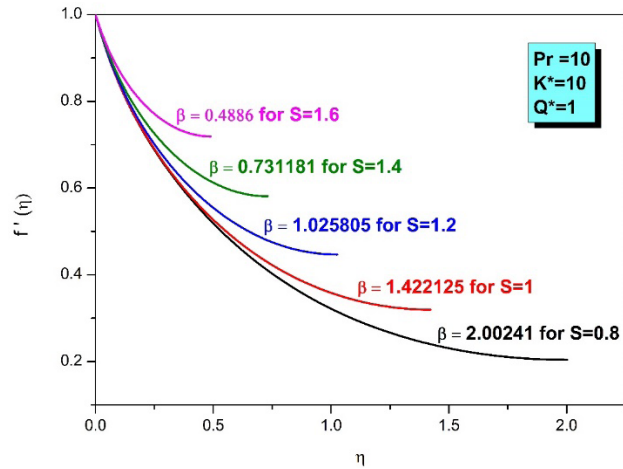


Figure 2. Velocity distribution for distinct  $S$  when  $K^*=10$ ,  $Pr=10$  and  $Q^*=1$ .

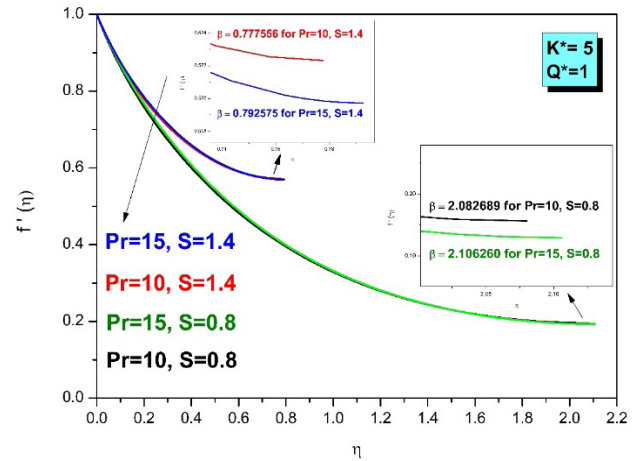


Figure 5. Velocity distribution for distinct  $S$  when  $K^*=5$  and  $Q^*=1$ .

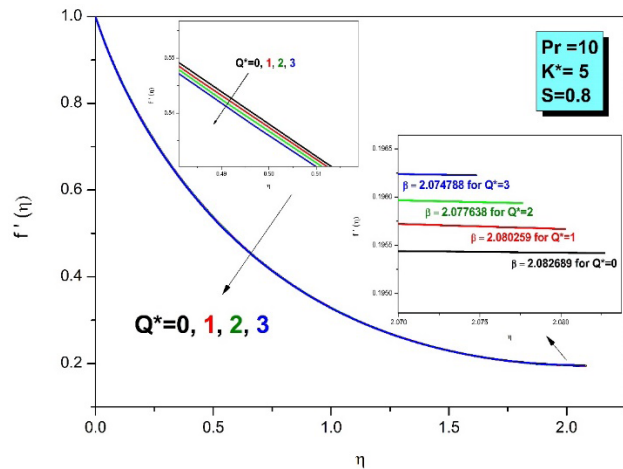


Figure 3. Velocity distribution for distinct  $Q^*$  when  $K^*=5$ ,  $Pr=10$  and  $S=0.8$ .

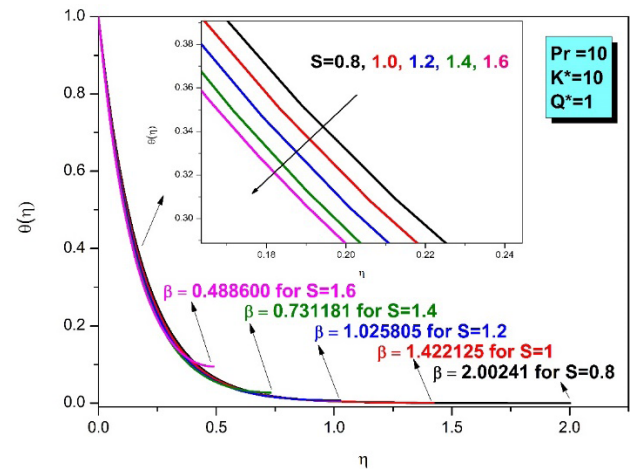


Figure 6. Thermal distribution for distinct  $S$  when  $K^*=10$ ,  $Pr=10$  and  $Q^*=1$ .

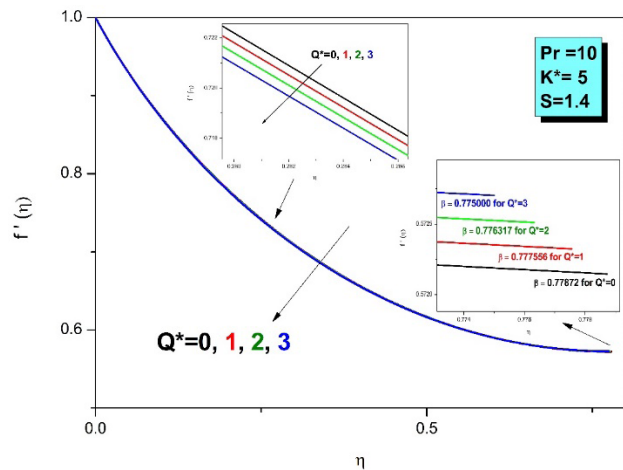


Figure 4. Velocity distribution for distinct  $Q^*$  when  $K^*=5$ ,  $Pr=10$  and  $S=1.4$ .

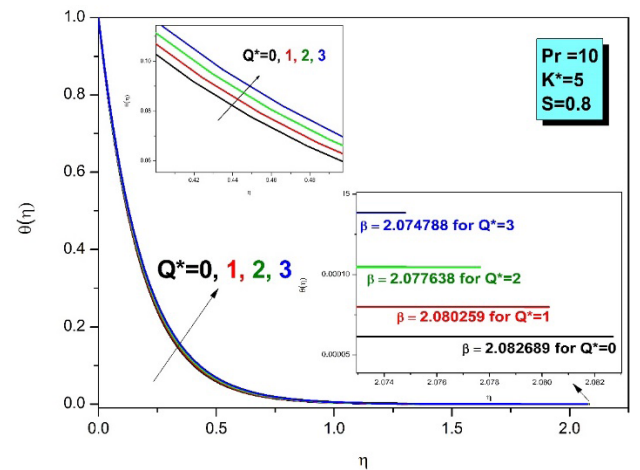


Figure 7. Thermal distribution for distinct  $Q^*$  when  $K^*=5$ ,  $Pr=10$  and  $S=0.8$ .

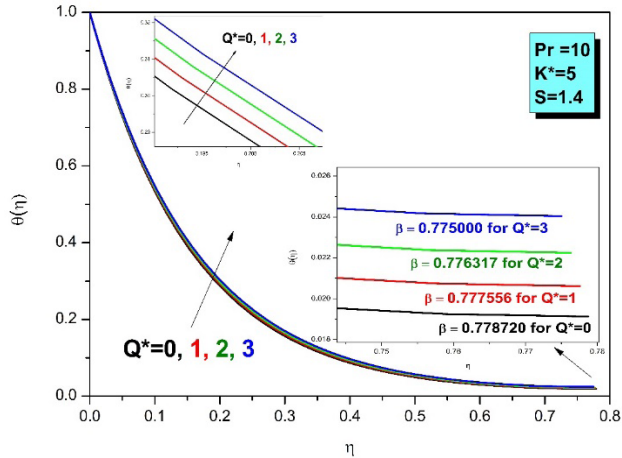


Figure 8. Thermal distribution for distinct  $Q^*$  when  $K^* = 5$ ,  $Pr = 10$  and  $S = 1.4$ .

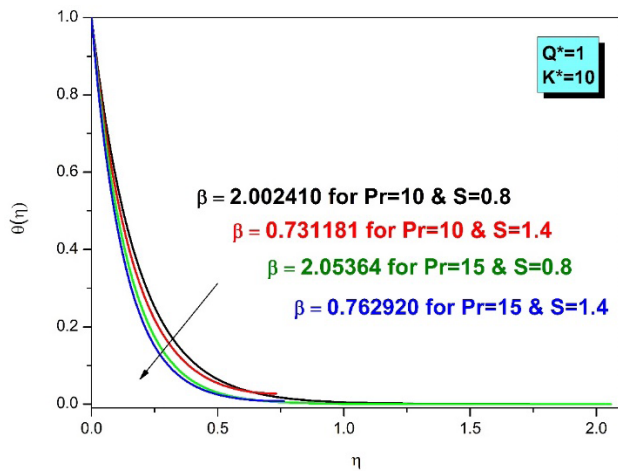


Figure 9. Thermal distribution for distinct  $S$  and  $Pr$  when  $K^* = 10$ , and  $Q^* = 1$ .

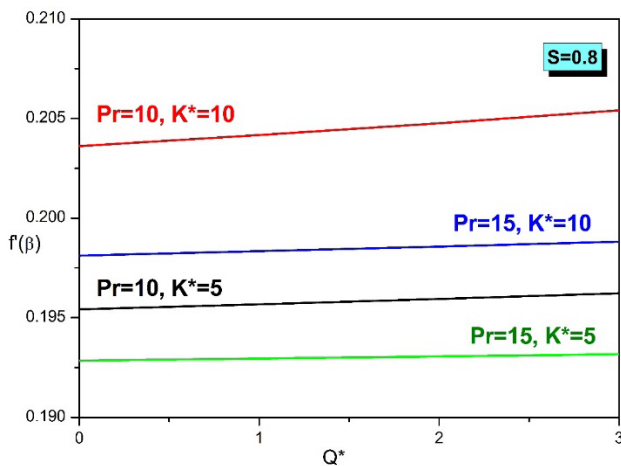


Figure 10. Free surface velocity vs  $Q^*$  for distinct  $K^*$  and  $Pr$  when  $S = 0.8$ .

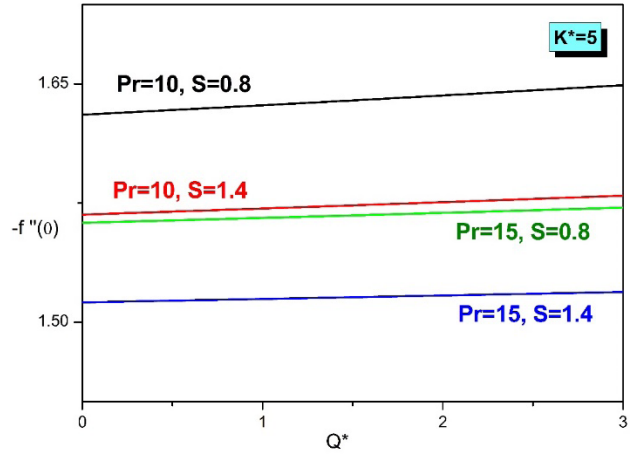


Figure 11. Frictional factor vs  $Q^*$  for distinct  $S$  and  $Pr$  when  $K^* = 5$ .

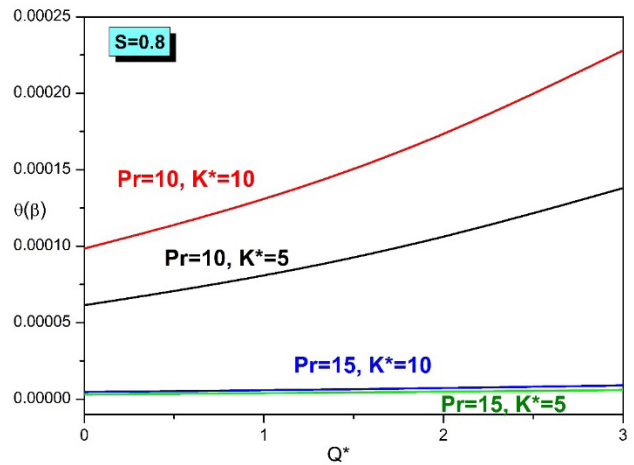


Figure 12. Free surface temperature vs  $Q^*$  for distinct  $K^*$  and  $Pr$  when  $S = 0.8$ .

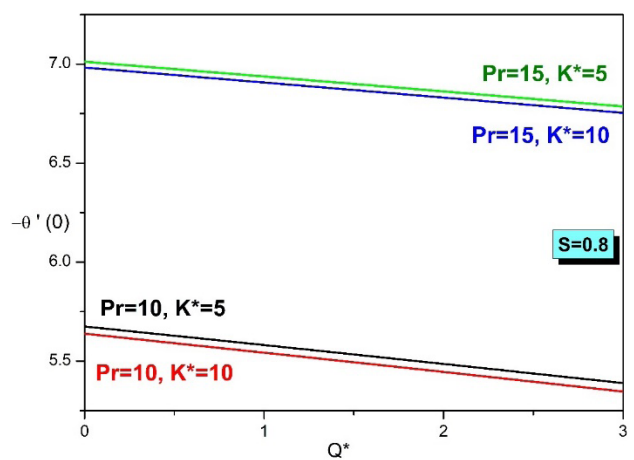


Figure 13. Wall temperature gradient vs  $Q^*$  for distinct  $K^*$  and  $Pr$  when  $S = 0.8$ .

velocity performance has been portrayed in Figure 5. The augment of the Prandtl number shows enhancement of the velocity performance near the boundary region and a reverse tendency is observed near the freestream region. In addition, the thickness of the thin film rises as the Prandtl number increases. On the other hand, the greater the value of  $S$ , the larger will be the velocity field. The high film thickness is noticed in case of lower values of  $S$  and larger values of  $Pr$ .

The influence of unsteadiness parameter on the temperature profile of the stretching sheet has been illustrated in Figure 6. It is noticed that the augment in  $S$  initially decreases the temperature performance, but an inverse trend forms near the freestream region. The smaller thin film thickness is noticed for larger  $S$  value.

The variation of the heat source parameter impacting on the thermal distribution in the boundary layer region has been presented in Figures 7 and 8 respectively for different values of  $S$ , by keeping  $Pr = 10, K^* = 5$ . The augment of the heat source parameter shows the enhanced nature of the thermal profile and the reduction in the thickness of thin film for both values of  $S$ . But reaching the freestream region is faster in case of  $S = 1.4$  than in case of  $S = 0.8$ .

The consequences of the simultaneous variation in the Prandtl number and the unsteadiness parameter on the temperature distribution of the stretching sheet has been described in Figure 9. It is noticed that, the augment in the Prandtl number improves the thickness of the thin film and decreases the thermal distribution. The convergence is observed near the freestream region.

The variation of the free surface velocity for diverse values of the heat source parameter has been captured in Figure 10 for different values of the Prandtl number and of the magnetization parameter while keeping  $S = 0.8$ . It is observed that the augment of  $Pr$  reduces the free surface velocity, while the rise of  $K^*$  and  $Q^*$  enhances the free surface velocity.

The variation of the frictional factor with respect to the heat source parameter have been exhibited in Figure 11 for different Prandtl numbers and unsteadiness parameters while keeping  $K^* = 5$ . The higher coefficient of skin friction is noted for smaller  $Pr$  and  $S$  values and larger heat source parameter.

The change of the free surface temperature for various heat source parameter has been presented in Figure

12 for different combinations of  $Pr$  and  $K^*$  by keeping  $S = 0.8$ . Clearly, the free surface temperature increases as the magnetization parameter increases and the Prandtl number decreases. A higher free surface temperature is noticed for larger  $Q^*, K^*$  and smaller  $Pr$ . The behavior of wall temperature gradient with varying  $Q^*$  have been portrayed in Figure 13. Here it is seen that the wall temperature gradient rises with rise in the Prandtl number and reduction in the magnetization parameter and the heat source parameter.

## 5.0 Conclusion

The main focus of this article is the numerical scrutinization of the thin film flow over an unsteady stretching sheet with magnetic field as well as heat source effect. The modelled equations have been further simplified and converted to ODE's and solved via shooting technique. The influence of the significant parameters has been explicitly deliberated using graphical representations. The main outcomes of the current simulations have been summarized as follows;

- The unsteadiness parameter and the heat source parameter reduce the thin film thickness.
- The velocity profile enhances with augment in unsteadiness parameter.
- Increasing the heat source parameter decreases the velocity profile near the boundary region and increases near the freestream region, whereas a reverse nature is observed in case of the Prandtl number.
- The thermal profile decreases near the boundary region and increases near the freestream region for increase in the unsteadiness parameter.
- The enhancement of the thermal profile is observed as the heat source parameter increases.
- As the Prandtl number falls and the magnetization parameter increases, the free surface velocity and temperature rise.

## 6.0 Acknowledgments

The author(s) are sincerely thankful to the Research Centre, M. S. Ramaiah Institute of Technology for constant encouragement and generous support.

## 7.0 References

1. Crane LJ. Flow past a stretching plate. *Zeitschrift für angewandte Mathematik und Physik ZAMP*. 1970 Jul; 21:645-7.
2. Andersson HI. An exact solution of the Navier-Stokes equations for magnetohydrodynamic flow. *Acta Mechanica*. 1995 Mar; 113(1-4):241-4.
3. Andersson HI, Aarseth JB, Dandapat BS. Heat transfer in a liquid film on an unsteady stretching surface. *International Journal of Heat and Mass Transfer*. 2000 Jan 1; 43(1):69-74.
4. Vajravelu K. Viscous flow over a nonlinearly stretching sheet. *Applied mathematics and computation*. 2001 Dec 15; 124(3):281-8.
5. Dandapat BS, Santra B, Vajravelu K. The effects of variable fluid properties and thermocapillarity on the flow of a thin film on an unsteady stretching sheet. *International Journal of Heat and Mass Transfer*. 2007 Mar 1; 50(5-6):991-6.
6. Khan NS, Islam S, Gul T, Khan I, Khan W, Ali L. Thin film flow of a second grade fluid in a porous medium past a stretching sheet with heat transfer. *Alexandria Engineering Journal*. 2018 Jun 1; 57(2):1019-31.
7. Safdar M, Khan MI, Taj S, Malik MY, Shi QH. Construction of similarity transformations and analytic solutions for a liquid film on an unsteady stretching sheet using lie point symmetries. *Chaos, Solitons & Fractals*. 2021 Sep 1; 150:111115.
8. Khan ZH, Khan WA, Qasim M, Shah IA. MHD stagnation point ferrofluid flow and heat transfer toward a stretching sheet. *IEEE Transactions on Nanotechnology*. 2013 Oct 25; 13(1):35-40.
9. Qasim M, Khan ZH, Lopez RJ, Khan WA. Heat and mass transfer in nanofluid thin film over an unsteady stretching sheet using Buongiorno's model. *The European Physical Journal Plus*. 2016 Jan; 131:1-1.
10. Ramana Reddy JV, Sugunamma V, Sandeep N. Effect of frictional heating on radiative ferrofluid flow over a slender stretching sheet with aligned magnetic field. *The European physical journal plus*. 2017 Jan; 132:1-3.
11. Krishanan R, Maity S, Dandapat BS. Unsteady flow of Casson liquid film on a stretching sheet with radiative heat transfer. *Surface Review and Letters*. 2020 Sep 25; 27(09):1950204.
12. Andersson HI, Valnes OA. Flow of a heated ferrofluid over a stretching sheet in the presence of a magnetic dipole. *Acta Mechanica*. 1998 Mar; 128(1-2):39-47.
13. Narayana M, Rani Titus LS, Abraham A, Sibanda P. Modelling micropolar ferromagnetic fluid flow due to stretching of an elastic sheet. *Afrika Matematika*. 2014 Sep; 25:667-79.
14. Jalili B, Sadighi S, Jalili P, Ganji DD. Characteristics of ferrofluid flow over a stretching sheet with suction and injection. *Case Studies in Thermal Engineering*. 2019 Sep 1; 14:100470.
15. Bhandari A, Husain A. Optimization of heat transfer properties on ferrofluid flow over a stretching sheet in the presence of static magnetic field. *Journal of Thermal Analysis and Calorimetry*. 2021 May; 144:1253-70.
16. Abel MS, Siddheshwar PG, Nandeppanavar MM. Heat transfer in a viscoelastic boundary layer flow over a stretching sheet with viscous dissipation and non-uniform heat source. *International Journal of Heat and Mass Transfer*. 2007 Mar 1; 50(5-6):960-6.
17. Abel MS, Mahesha N. Heat transfer in MHD viscoelastic fluid flow over a stretching sheet with variable thermal conductivity, non-uniform heat source and radiation. *Applied Mathematical Modelling*. 2008 Oct 1; 32(10):1965-83.
18. Zheng L, Wang L, Zhang X. Analytic solutions of unsteady boundary flow and heat transfer on a permeable stretching sheet with non-uniform heat source/sink. *Communications in Nonlinear Science and Numerical Simulation*. 2011 Feb 1; 16(2):731-40.
19. Majeed A, Zeeshan A, Noori FM, Masud U. Influence of rotating magnetic field on Maxwell saturated ferrofluid flow over a heated stretching sheet with heat generation/absorption. *Mechanics & Industry*. 2019; 20(5):502.
20. Aslani KE, Mahabaleshwar US, Sakanaka PH, Sarris IE. Effect of partial slip and radiation on liquid film fluid flow over an unsteady porous stretching sheet with viscous dissipation and heat source/sink. *Journal of Porous Media*. 2021; 24(11).